4. STREAM MORPHOLOGY AND DOWNSTREAM HYDRAULIC GEOMETRY RELATIONS FOR BANKFULL WIDTH

Mario A. Jiménez[1], Jaime I. Vélez[1] & Luis A. Camacho[2]

[1]Universidad Nacional de Colombia –Medellín. Medellín – Colombia

[2]Universidad de los Andes. Bogotá – Colombia

ABSTRACT

Since the pioneered findings by *Leopold and Madoc*k [1953], hydraulic geometry (HG) has been applied to support multiple engineering applications. However, the sources of scattering on the worldwide derived relationships at a station and downstream HG, are still being the research interest of fluvial morphologists. In this work, downstream HG for bankfull width is analyzed from the point of view of the morphological settings of 123 stream reaches located throughout several climatological regions of Colombia and Venezuela (South America). Bedforms settings were defined based on the extension of the Montgomery and Buffington (1997) morphology classification framework, posed by Flores *el at*. [2006]. The proposed methodology was applied using digital elevation models as well as satellite images taken from Google Earth. Planform features including curvature radius, amplitude, and bend length, were also estimated from detailed stream axis courses digitalized from the available satellite images along the stream corridor. The procedure allowed the definition of three HG universal classes, corresponding to channels classified as transport-limited, supply-limited and braided, and whose scatter around the obtained main trend did not show to be systematically influenced by climatological settings. Rather, the confinement degree assessed in terms of the bend length to width ratio (L_b/W) showed to be an explanatory variable of the quasi-universal pattern in the transport-limited category, allowing to propose a fourth HG universal class. Further work must be carried out for the supply-limited systems, since this universal class appear to have high scattering and also shows a likely independence of the L_b/W ratio.

Key words: *hydraulic geometry, bankfull width, stream morphology*.

4.1 INTRODUCTION

Since the pioneered findings by *Leopold and Madock* [1953], hydraulic geometry (HG) has been applied to support multiple engineering as well as research applications worldwide. These include preliminary channel-dimension computations in stream restoration programs, ranging from planview variables assessment, such as channel width, meander wavelength and curvature radius [*Shields Jr. et al.*, 2003; *Rinaldi and Johnson* 1997], to bedform features identification, such as pool-to-pool spacement characterizing stream reaches likely to have pool-riffle and step-pool morphological types [*Myers and Swanson*, 1997; *Jiménez and Wohl*, 2013].

Hydrological modeling is also supported by HG theories when parameterization of cross section shape is required for distributed flood-routing purposes. Several works have incorporated these HG techniques [*Orlandini and Rosso*, 1998; *Vélez*, 2001; *Mejia and Reed*, 2011; *Neal et al.*, 2012] whose common feature is the use of a reference geometry condition commonly associated with a representative discharge. Definition of either single channel geometry *i.e*., rectangular or trapezoidal shape, to more complex channel-floodplain geometries, becomes an issue of interest mainly because of its influence on the travel time response along a stream reach and the entire drainage network.

It has been shown that bankfull width, one of the classical variables for which downstream hydraulic geometry has been derived, is an appropriate scale factor (or reference condition) when comparisons among stream-morphological processes are the main focus. The rhythmical self-formed bedforms along step-pool and pool-riffle stream types [*Montgomery and Buffington*, 1997] have been expressed by morphologists as dimensionless bankfull width units. Like bedforms, planforms have been widely expressed as channel width units, as it is the case of either the curvature-to-width, wavelength-to-width or amplitude-to-width ratios for meander bends, and for stream midsection axis [*Leopold and Wolman*, 1960; *Williams*, 1986; *Nicoll and Hickin*, 2010]. Besides, bankfull width appears to be useful for making morphological assessments that are scale-independent. Reliability on estimating stream-bend features is a real issue when sampling intervals between1.5 to 4 channel width equivalents [*Ferguson*, 1975; *Milne*, 1983; *Howard and Hemberger*, 1991]. Similarly, *Zimmerman et al.* [2008] posed a scale-free method to objectively identify pool and step units along step-pool profiles where the method parameters are all expressed as fractions of bankfull width.

Hydraulic geometry limitations are also well documented, and have been identified mainly motivated by the worldwide variations in the HG exponents, as well as the scattering obtained around the main fitted trends used to describe either, at-station, or downstream hydraulic geometry. Formally, those variations have been explained in terms of multi-scaling and universality [*Dodds and Rothman*, 2000]. The former refers to the invariant dependence that a variable could have under variations of some key independent scale factors, and the latter makes reference to the underlined mechanisms and generic processes which lead to such scaling pattern. Deviations from universality in HG, appears to be related to local factors including bank material strength, sediment supply, asymmetrical cross-sectional geometry imposed by planforms, local lithology and geology settings, and differences in climatological driving forces [*Park*, 1977; *Burns*, 1998; *Dodov and Foufoula-Georgiou*, 2004; *Wohl*, 2010; *Parker et al.*, 2007; *Eaton and Church*, 2007]. Hence, under an appropriate universal class definition, sources causing such deviations can be better isolated and understood.

Burns [1998] posed that hydraulic geometry relations developed after distinguishing stream types could lead to reductions of scattering, a statement later confirmed by *Vianello and D'Agostino* [2007] based on distinctions on the bankfull width adjustment of colluvial cascades, and step-pool morphologies. *Parker et al.* [2007] showed for gravel-bed rivers that hydraulic geometry for bankfull width, bankfull depth, and slope, follow simple scaling laws, although deviations from universality were found explicitly related to the underlying physics including banks strength, sediment supply (gravel supply), and transport capacity. Such formulation was developed taking into account a wide range of watershed sizes, stream sizes, and sediment sizes expressed dimensionless.

In this work, stream morphology is explored allowing the distinction of universal classes of downstream hydraulic geometry for bankfull width in single thread channels located in different climatological regions along Colombia and Venezuela (South America), having a wide scale range, *i.e.* variable watershed area. Morphological types were defined according to the Montgomery and Buffington classification system, adapted by *Flores et al.* [2006] by incorporating stream power as a discriminatory variable together with reach slope, in order to distinguish step-pool morphologies from cascade systems, as well as pool-riffle from plane bed systems. Planform features were also used as morphological descriptors in order to explain deviations from universality.

4.2 DATA SET AND METHODS

A set of 123 stream reaches was selected within Colombian and Venezuelan territories (Figure 4-1) at places where high definition Google Earth satellite images spots were available. The set of data covers a wide watershed area interval ranging from 0.66 km^2 to 115,295 km^2, and includes cascade, step-pool and pool-riffle stream morphological types according to the *Montgomery and Buffington* [1997] classification system. Additionally, a total of 14 braided systems completed the sample.

The selected reaches are also spread out along different hydro-climatological regions distinguished in terms of their homogeneity, according to previous regionalization studies conducted in Colombia [*UNALMED et al.*, 1999]. As a result of a multiscaling peak flow analysis in those regions, equations in the form $Q_{Tr} = CA^q$ are available for different frequencies. Table 4-1 summarizes the number of reaches available within each region as well as the coefficients and exponents corresponding to 2.33-year and 10-year recurrence intervals floods.

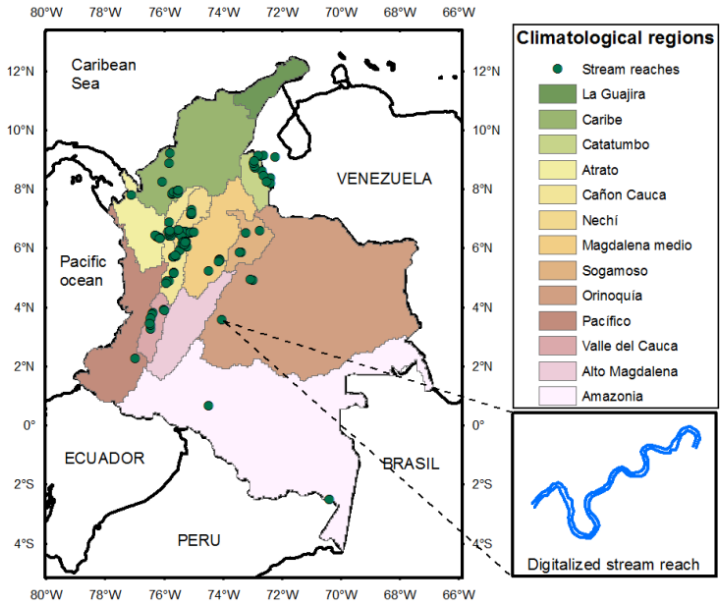

Figure 4-1. Study area location and data spreading thorough it

Table 4-1. Coefficients (C) and Scaling exponents (q) of floods for every climatological region and available data

Climatological region	Number of reaches	2.33 reccurrence interval years parameters		10 years reccurrence interval parametres	
		q	C	q	C
La_Guajira (Z1)	0	0.1630	58.3500	0.0150150	254.8200
Catatumbo (Z2)	13	0.6227	4.2055	0.5221	13.9056
Caribe (Z3)	11	0.6633	2.4184	0.5708	7.2137
Nechi (Z4)	15	0.8327	0.9261	0.7722	1.8773
Atrato (Z5)	8	0.8998	0.6575	0.8275	1.3673
Sogamoso (Z6)	4	0.8927	0.2242	0.8573	0.4499
Magdalena_Medio (Z7)	33	0.7422	1.7074	0.7106	3.1485
Canon_Cauca (Z8)	18	0.6542	2.5691	0.6191	4.7212
Valle_del_Cauca (Z9)	9	0.5781	3.6898	0.5305	7.2007
Alto_Magdalena (Z10)	0	0.8633	0.5755	0.8189	1.1416
Orinoquia (Z11)	3	0.3971	45.1081	0.3433	94.8427
Pacifico (Z12)	1	0.5656	11.8639	0.5549	17.1866
Amazonia (Z13)	2	0.7412	4.9150	0.6590	11.5100

4.2.1 Morphological features

The watershed area, A, draining at each stream reach point of analysis was calculated using several available digital elevation models -DEM-, depending on the stream size, and the availability of a stream network which could be used to derive a flow direction map. The 1 and 3 seconds arc pixel size SRTM maps [*Farr et al.*, 2007] were used for those cases where a stream network was available at local environmental agencies databases. Otherwise, the USGS HydroSHEDS [http://hydrosheds.cr.usgs.gov/index.php] mapping products were used. The reach slope, S_0, was estimated as the drop height to the reach length ratio, sampling the elevation of the upstream and downstream reach edges directly from the DEM.

Using the satellite images, the borders of the selected reaches were digitalized along the path that suggested the higher geomorphically-effective discharge (see Figure 4-2). For lowland reaches, the bank-stage definition did not represent a so hard goal as for those reaches located in the upper zones given higher canopy interferences, which in some cases avoided the river borders visualization. Nevertheless, more than 90% of the digitalized streams had a reach length higher than 15 times the mean channel width in order to ensure more reliable width estimation.

Figure 4-2. Stream reach borders digitalization and transects extraction for width estimation

A set of AutoCAD Visual Basic macros were developed to automatically derive the reach-averaged width, W, and its corresponding standard deviation, σ_W. Figure 4-2 illustrates the procedure, in which the first step consists of resampling the downstream axis using a regular spacing fixed to a close value of the expected W. Subsequently, perpendicular transects are defined along the resampled axis intersecting the digitalized river borders, in turn, allowing the estimation of the corresponding width value at each axis node.

The radius of curvature R_c along stream paths has been pointed out as a quantitative descriptor of meander bends, and its relation to the stream width has been highlighted for several stream corridor settings. The relationship between R_c and W is almost linear as shown in the empirical equations derived by *Leopold and Wolman* [1960] and later by *Williams* [1986]. Therefore, R_c was introduced in the analysis to support the bankfull width HG assessment, especially for those cases having high uncertainty due to the riverine vegetation interferences during the river bank digitalization procedure.

In this work, a method is proposed to make the curvature measure independent of how fine or irregular the digitalized axis is. This is because the downstream axis is represented by a set of (x,y) points that are totally dependent on the digitalization procedure. Additionally, instead of using the mean curvature radius R_c, we used the median radius R_m in order to avoid overestimations biased by straight segments in the downstream axis.

To obtain R_m, the downstream axis is iteratively re-meshed using a regular spacing ΔX_i within the interval $[0.01W - 10W]$, where W is the reach-averaged bankfull width previously estimated. A radius of curvature is then assigned to every three consecutive points along the new axis, thus

making an estimation of the median radius that corresponds to a given mesh resolution. When the entire mesh interval is sampled using incremental values of 0.01W, a diagram of ΔX *versus* R_m can be set as shown in Figure 4-3. The first maximum local variance and the second minimum local variance of the obtained diagram allow the identification of a W fraction for which the median radius estimation remains almost invariant. Such fraction was used to assess the R_m value corresponding to each stream reach.

Once R_m is estimated for every stream reach, the median reach amplitude *Amp* was also calculated. The method proposed by *Dodov and Foufoula-Georgiou* [2004] was applied to split the entire stream axis into bend units for which an amplitude a_i was then estimated. The method first creates a secondary axis as a result of filtering the set of (x,y) pairs making up the downstream axis. The corresponding window size used is the median curvature radius previously estimated. Intersections between the original and secondary axis define the boundaries of the individual bends characterizing the reach, so that a_i can be assessed as well as the median value as a representation of the analyzed reach.

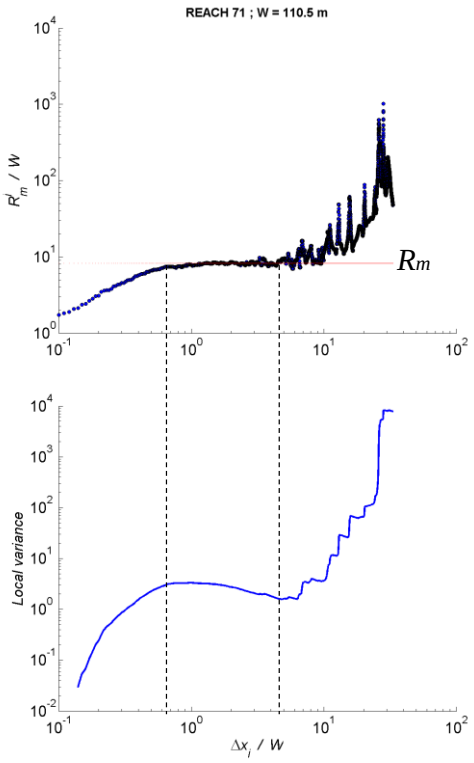

Figure 4-3. Stream curvature variation with mesh size and median values estimations based on maximum and minimum local variances

4.2.2 Reach-morphology type

In order to implement an objective morphological classification method for the entire data set, taking into account the lack of detailed hydrological and sedimentology information at every reach, we used the cross-validated classification tree proposed by *Flores et al.* [2006] -see Figure 4-4-. This method is based on the reach slope S_0, in order to distinguish supply-limited and transport-limited channels, and the index of specific stream power $S_0A^{0.4}$, to distinguish step-pool from cascade reaches in the former category and pool-riffle from plane bed reaches in the latter.

It must be noted that such classification system is a simplification of the pioneer *Montgomery and Buffington*'s [1997] process-based fluvial classification system, in which only the alluvial types cascade (C), step-pool (SP), pool-riffle (PR) and plane bed (PB) are considered.

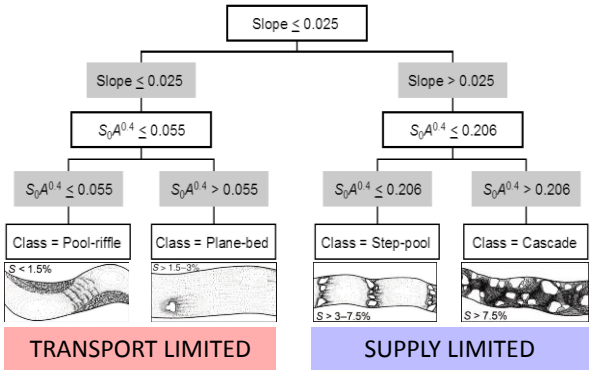

Figure 4-4. Stream morphology classification framework proposed by Flores *et al.* (2006)

4.3 RESULTS AND DISCUSSION

4.3.1 Reach-averaged features

The width-area plot using the calculated widths is shown in Figure 4-5a. A high scattering degree can be observed, even though a reach-averaged value was derived. According to previous works, contributions to scattering could be explained by, either the use of the watershed area as the independent variable or the differences between the morphological settings of the stream reaches [*Burns*, 1998]; the scale-dependent HG exponents on the increase of channel asymmetry downstream induced by scale-dependent fluvial instability [*Dodov y Foufoula-Georgiou*, 2004]; the spread of data throughout the study area and thus the variability of the hydrological controlling factors; local factors including sediment supply and bank material strength [*Parker*, 2007]; and the inherent uncertainty of the data.

It becomes clear that a unique power law relationship, as shown in Figure 4-5a, is not appropriate for making new width predictions. By using this relationship, overestimations up to 188% and underestimations of 87% were obtained for sampled width values.

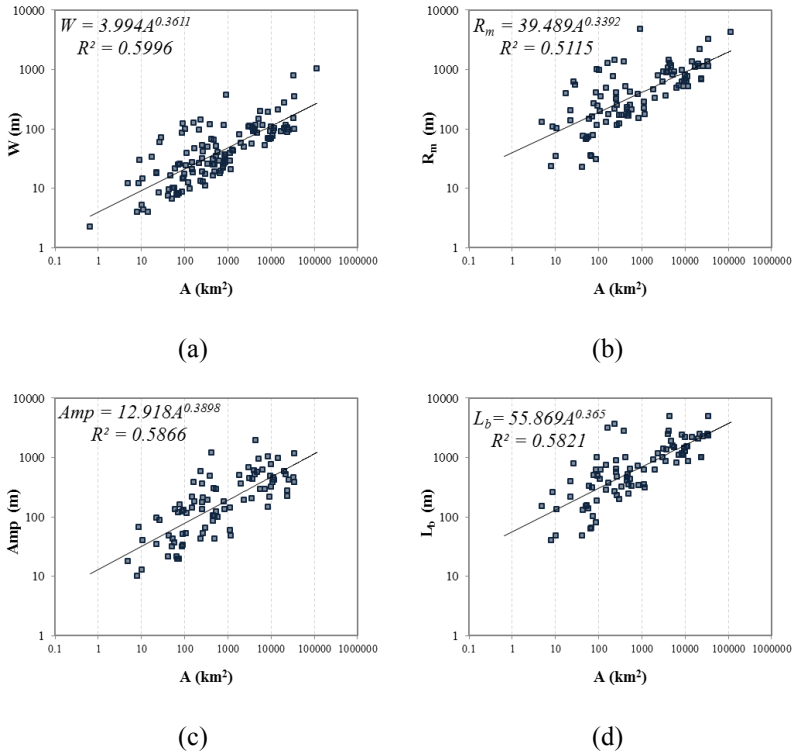

Figure 4-5. Reach-averaged width (a), curvature radius (b), bend amplitude (c) and bend wavelength (d) related with watershed área

A similar scattered pattern was found when the median curvature radius -R_m-, amplitude -*Amp*- and bend wavelength -L_b- were plotted against the watershed area (Figure 4-5b, c and d). Such correspondence was found to be underlined by the strong relationship between those variables and *W*, as display in Figure 4-6a. It turns out interesting that such linearity not only describes the available low-gradient reaches but also the entire data set.

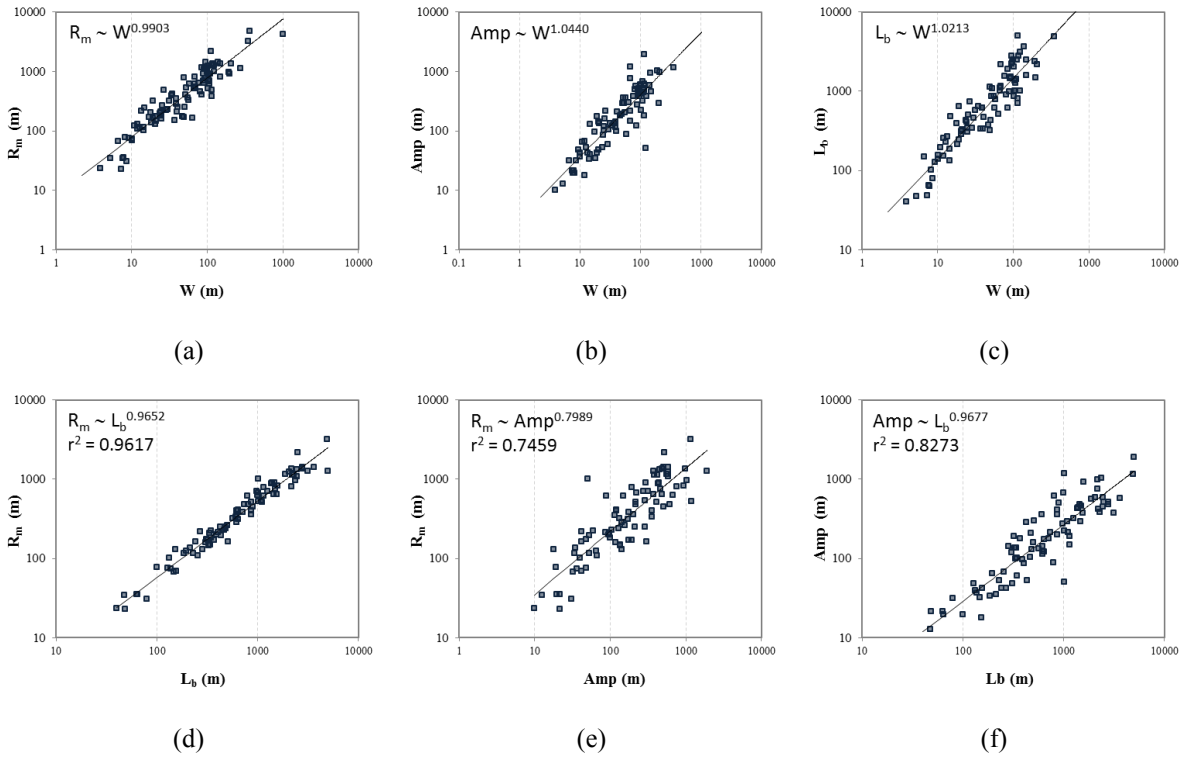

Figure 4-6. Linear trends among planform features in relation to channel size –a, b, c- and mutual adjustments between radius, amplitude and stream wavelength –d, e, f-

The calculated ratio R_m/W ranges from 2.56 to 19.35, a wide interval when compared to that reported by *Leopold and Wolman* [1960], *Williams* [1986], and *Alvarez* [2005]. Curvature radius is considered an important feature, taking into account that both, bend wavelength, and amplitude assessment are based on a previous estimation of R_m. Hence, in order to verify possible bias caused by the method to estimate R_m, the obtained results were compared with the method proposed by *Alvarez* [2005] (denoted as the reference method), for which the radius of curvature at any point along a meander bend can be assessed by,

$$R = \frac{\left[1+\left(\frac{dy}{dx}\right)^2\right]^{3/2}}{\frac{d^2y}{dx^2}} \qquad 4\text{-}1$$

Thereby the mean curvature radius R can also be estimated. Again, the median value was used instead of the mean value, for the same reason regarding extreme R values associated with straight

portions of the stream axis. Additionally, equation (4-1) was expressed numerically using finite differences in order to allow the application of the method for an entire stream axis instead of a well-defined meander bend.

Both methods appear to be dependent on the stream-reach axis resolution as illustrated in Figure 4-7, where the variability of the median radius of curvature of four different reaches is compared. To effectively make comparisons, the radius obtained by the reference method was calculated for a resolution corresponding to the centered mesh-size, a value within the sill obtained by the proposed method. Comparisons between both R_m - W trends, show that the reference method yields to higher radius estimations as well as to higher scattering. For this reason, the proposed method is advantageous since it is scale free and it is stable for meander bends or stream segments. Moreover given the strong correlation obtained, R_m could be seen as a surrogate estimator of W when high detailed vector data is available..

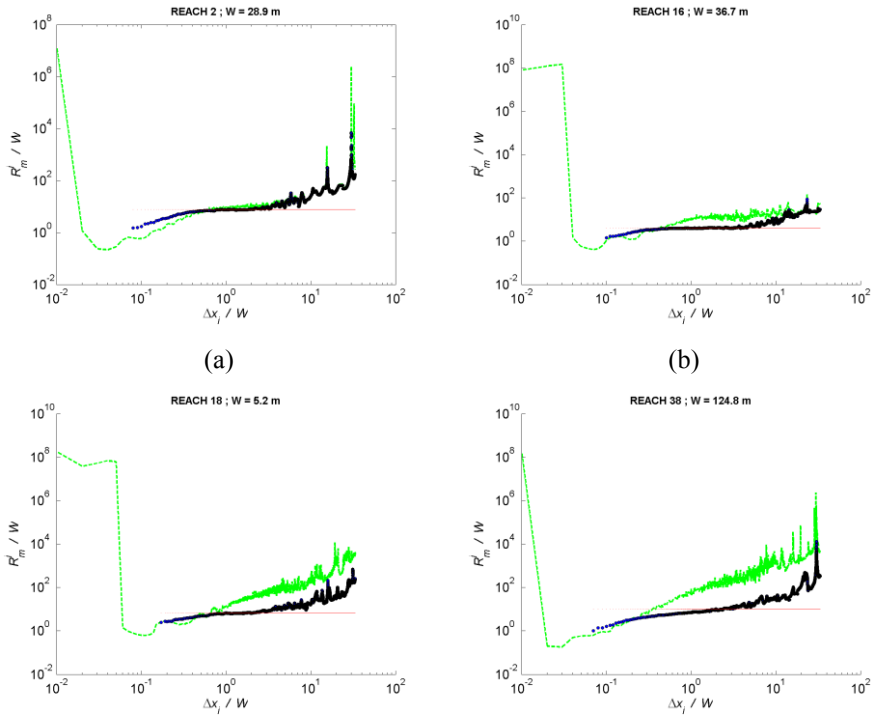

Figure 4-7. Dependence of curvature on the mesh axis size and comparisons between estimations using the proposed method (dark blue dots) and the reference method by Alvarez (2005) –dashed green lines-

The mutual adjustments among the planform features R_m, *Amp* and L_b, showed in Figure 4-6, revealed a close R_m-L_b interdependence which suggest that this variables could allow to explain dispersion in the R_m-W and L_b-W diagrams (Figure 4-6a and Figure 4-6e). Figure 4-8 shows that values above and below the fitted mean trends, define distinguishable groups for the L_b to W ratio (Figure 4-8b) or the R_m to W ratio (Figure 4-8f). Conversely, amplitude (Amp/W ratio) does not allow making distinctions (Figure 4-8d and Figure 4-8h) of data, perhaps because amplitude can be seen more as an external restriction than a result of auto-adjustment of the stream.

The previous work by *Nicoll and Hickin* [2010] carried out using confined meandering rivers data, posed the influence of valley confinement on the deviation in the L_b/W and R_m/W ratios from typical values reported for freely meandering rivers. According to their results, the higher the confinement degree, the higher ratio L_b/W and R_m/W. Such finding supports the R_m/W ratios obtained here, whose wide variation is linked to the L_b/W ratio which in turn seems to explain indirectly the confinement patters along a stream reach. It must be also noted in Figure 4-8b that the variability for the L_b/W ratio above the mean R_m-W trend is high. Hence, since such behavior is not biased by the sample size, *i.e*. 45 reaches above and 42 reach below, the reasons are more likely related to the heterogeneity in the natural controls on the migration processes for those stream reaches, including steep hillslopes walls, local lithological controls, and differences on bank material strength.

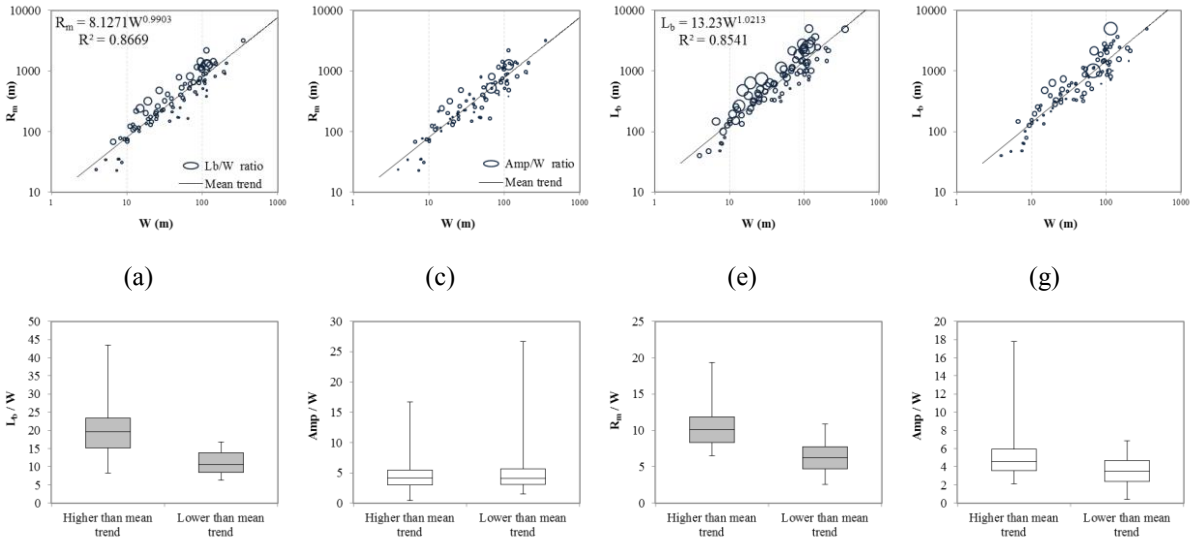

Figure 4-8. Mutual adjustments between planform geometry variables

4.3.2 Hydraulic geometry morphologically influenced

A new width-area plot was set using the reach-morphology segregation obtained by applying the *Flores et al.* [2006] classification scheme. As can be noticed in Figure 4-9a, an important amount of data scattering can be attributable to the cloud of (A, W) pairs corresponding to braided channels which in turn define the highest W values within the sampled watershed areas. This finding was pointed out in the early work by *Kellerhals and Church* [1989] and it was related to the high sediment supply that characterizes braided systems. More recently, *Parker et al.* [2007] carried out a more detailed analysis in gravel-bed rivers, finding that higher gravel yield leads to widening channel processes. In their work, such sensitivity was also highlighted as a contribution to deviations from universality on the bank-full width HG of gravel-bed rivers.

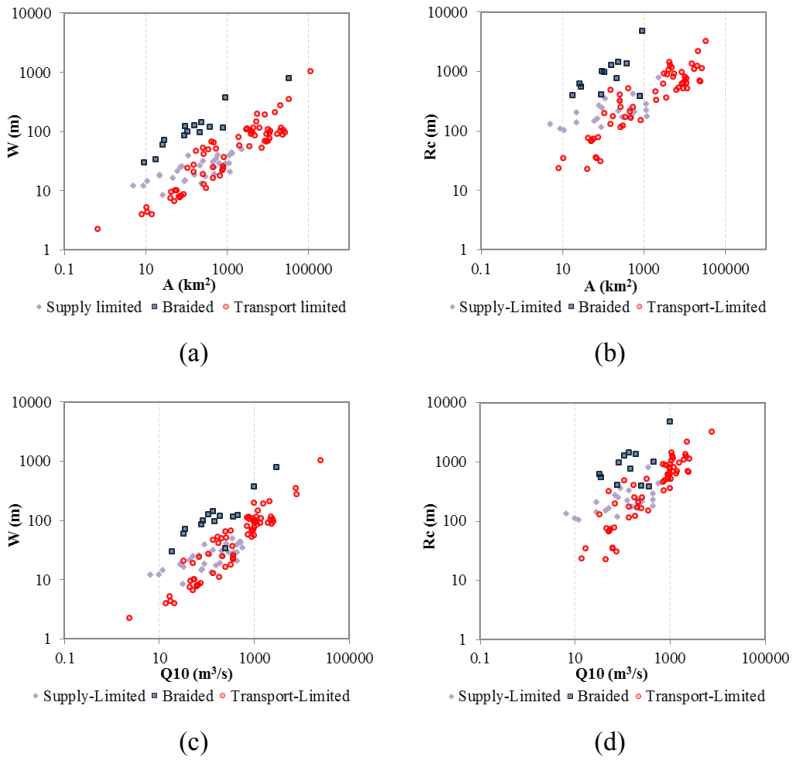

Figure 4-9. Reach-averaged width (a), curvature radius (b), bend amplitude (c) and bend wavelength (d) related to watershed area, after a stream classification using the framework by Flores *et al.* (2006)

After using the morphology classification method adopted here, ten braided-dominated reaches were classified as plane-bed morphologies, three as step-pool and one as pool-riffle morphology. Overlapping of the bed-slope ranges was identified as the primary reason for the classification tree

to be erroneous, as well as the fact that the method was derived for single-thread channels, thus making it less reliable for braided systems. Variations of bed slope S_0 are shown in Figure 4-10 for each morphological type after the classification scheme was applied. Blank boxes are related to S_0 variation in the available reaches, and filled boxplots are the corresponding intervals reported by *Flores et al.* [2006]. Because of the effect caused by slope overlapping, reaches having braided morphology (according with visual classification) were separately treated in the subsequent analysis.

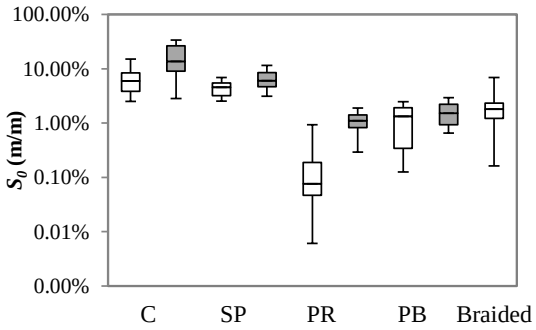

Figure 4-10. Channel slope variation. Blank boxes correspond to values found using the available data in this study. Filled boxes correspond to intervals by Flores et al. (2006)

Like braided systems, morphologies in the supply-limited category (step-pool and cascade types) suggest a differentiable trend when compared to that followed by the transport-limited reaches (plane-bed and pool-riffle types). Unfortunately, it was not possible to distinguish a unique pattern between the pool-riffle and the plane-bed types, nor between the cascade and step-pool types.

As expected, the radius-area plot also displays analogous segregation of the data (Figure 4-9b), thus supporting the insights that the defined morphological categories can effectively be grouped separately. Besides, a confirmatory link was found between the preferential data arrangement in the R_m-W diagram, related to the L_b to W ratio, and those reaches having clear signatures of free meandering processes and thus less confinement degree, according with the available aerial images (see Figure 4-11). Besides, it is noticeable that reaches having a L_b/W ratio below 13.23, correspond not only with those migratory reaches, but also with some supply-limited channels (and even braided), that appear to satisfy the same threshold, thus motivating further analysis in subsequent work regarding their definition.

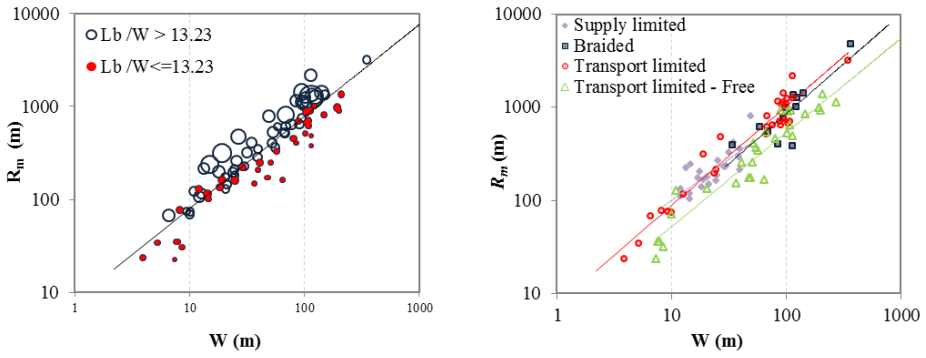

(a) (b)

Figure 4-11. Quasiuniversality of the radius to width ratio caused by the confinement dregree expressed in terms of the L_b/W ratio (a), and consistency with stream reaches having free meandering planforms (b).

In order to make an evaluation of the effect of using the watershed area as a surrogate of a formative discharge, the flood Q_{10} was introduced as the independent variable (Figure 4-9c and Figure 4-9d). Although there is a rearrangement of the data, the morphological categories remain having more influence on the general trends obtained, than that associated with the choice of the independent variable.

Further inspection was made separately for each morphological category as shown in Figure 4-12. All categories, but the braided, did not display evidence that allowed distinguishing climatological preferences regarding how the data was grouped. However, it must be consider that the number of reaches for the braided category does not give enough statistical support to establish a climatological-zone segregation. Conversely, a view of the HG pattern within each climatological region suggests differentiable classes in the zones Cañon del Cauca, Nechí, Magdalena Medio and Catatumbo. Those classes (represented with the size of the bubbles in Figure 4-13) were expressed in terms of the specific stream power computed for every reach, since this variable has been posed as a discriminatory variable between morphological types. In the rest of the zones it was difficult to make any differentiation either because of the few available data (Sogamoso and Valle del Cauca) or because of the lack of wide watershed area intervals.

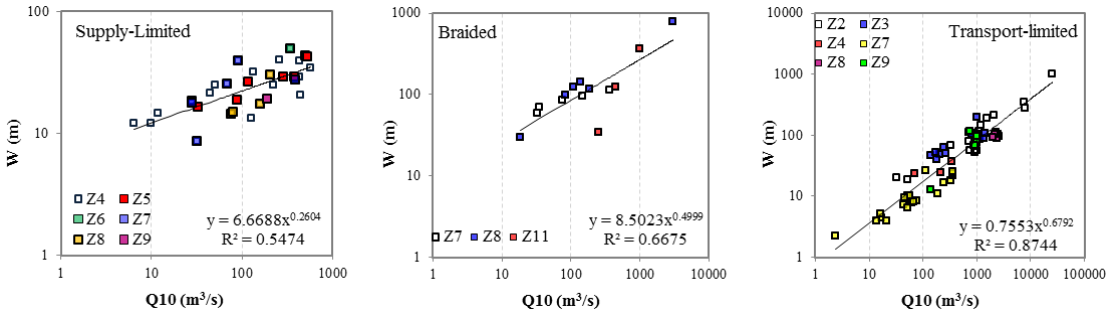

Figure 4-12. Hydraulic geometry trends using the representative discharge Q10 as independent variable and considering climatological regions to seek for possible data segregation

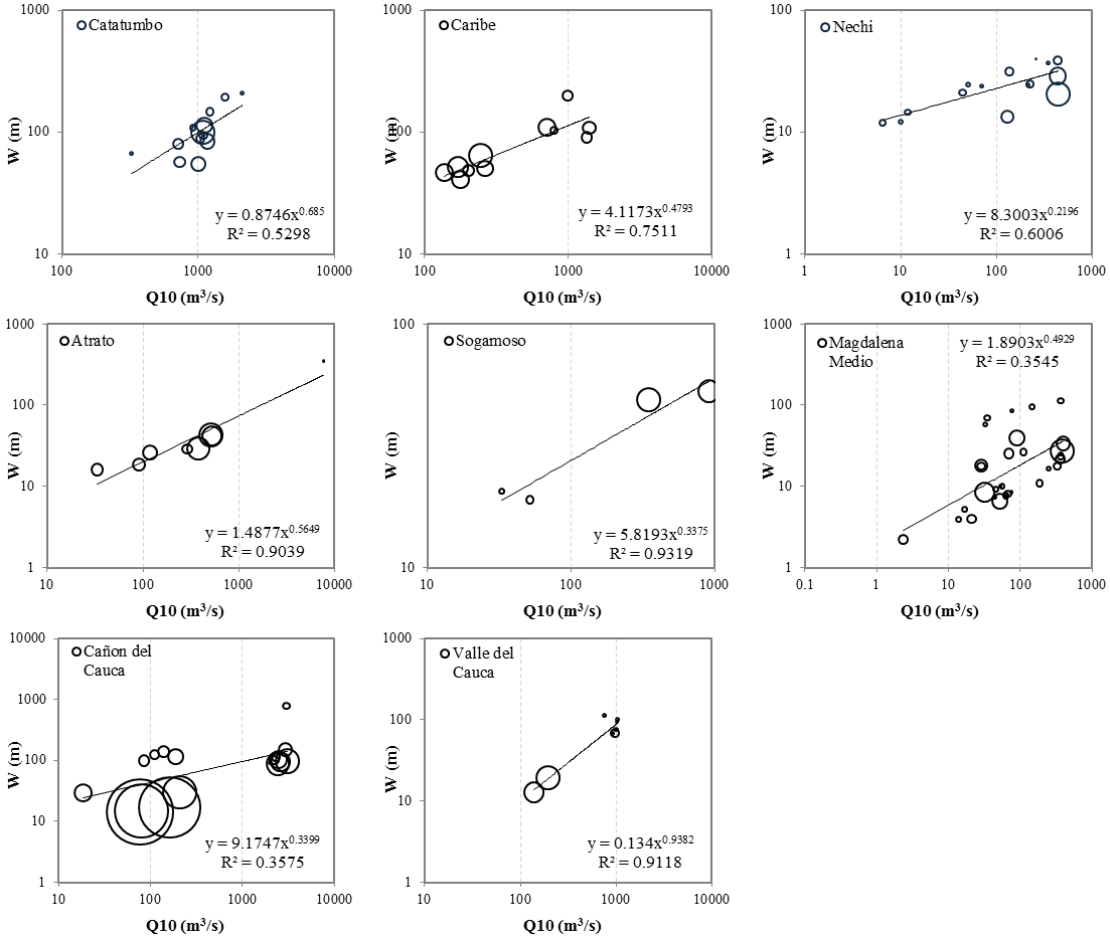

Figure 4-13. Hydraulic geometry trends within each climatological region (Bubble size represent the magnitude of specific stream power)

4.4 CONCLUSIONS

Four hydraulic geometry classes for bankfull-width were here defined, and their differentiation was support by the analogous pattern found in terms of the radius of curvature. Such finding gives supported by the statement that different morphological types lead to differences in the HG pattern for channel width *W*. Additionally, correlations between channel width and the mean curvature radius suggest that bankfull-width HG accounts implicitly for secondary factors related with planform. Specifically, contributions to the quasi-universality in the HG classes were found to be related with the confinement degree of the analyzed stream reaches, which was assessed in terms of the L_b/W ratio. Figure 4-14 displays the obtained hydraulic geometry relationships, including the correspondent empirical relation for those transport-limited reaches having clear channel migration zones as well as L_b/W values less than 13.23.

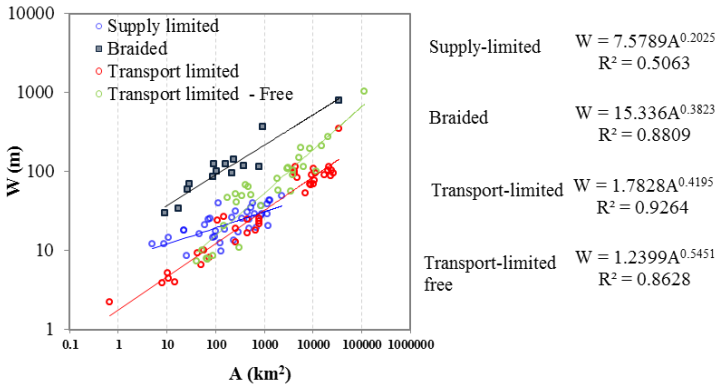

Figure 4-14. Downstream hydraulic geometry relationships obtained for bankfull width

The interval 1.21*W*- 4*W* for which the curvature radius showed to be invariant regardless the axis mesh-size, agrees with the former work by *Ferguson* [1975] and *Howard and Hemberger* [1991], where values of 1.5-2 and 2-4 channel width where respectively reported as satisfactory for establishing a scale-free method to characterize meandering rivers. Such correspondence not only validates the results presented here, but gives further insights regarding the selection of an adequate DEM resolution for morphological analyses purposes. Besides, the strong relationship R_m-*W* obtained, showed to be generalizable beyond the lowland streams for which meander bends have been intensively studied, since together with the transport-limited reaches, braided systems, as well as those belonging to the supply-limited category also exhibit such linear behavior.

Deviations from the mean trend in the DHG relationships were found systematically related with lateral downvalley constraints, either by valley confinement or bank-material resistance, which prevent a reach to develop a free channel migration zone. The L_b to W ratio was the planform feature that allowed making those distinctions based on a threshold around 11-14. Consistently, 78% of the transport-limited reaches having L_b/W values less than 13.23, are related to those for which evidences of an active channel migration zone, including oxbow lakes, chutes and main channel drifts revealed by the available historical imagery, were identified. Nonetheless, it must be mentioned that further analysis needs to be carried out in order to establish the natural controls on confinement, since it comes from either steep adjacent hillslopes or high resistant bank materials.

An apparent advantage of the methods proposed here to quantify planform geometry features is that they require less detailed vector data for a specific stream corridor or, drainage network. Moreover, the wide reach settings conforming the used data set, suggest that those methods can be easily replicated. It is worth implementing a future application allowing hybrid morphological assessments using both raster data and vector data as a surrogate when the former does not have an appropriate resolution when compared with the fluvial system size.

Climatological factors have been pointed out as explanatory causalities of the scattering of hydraulic geometry relationships. Nonetheless, there was not found any systematic grouping of the data in the W vs A diagram, neither when these were separated within different climatic environments, nor when the surrogate variable A was replaced with the 10-year recurrence interval flood.

4.5 ACKNOWLEDGMENTS

Special thanks to COLCIENCIAS for the founding provided during the first three years of the first author's *Ph. D* program. Also to the Universidad Nacional de Colombia for providing the software licenses on which methods were implemented.